

energies of 10.4 A MeV and impact parameters approximately equal to  $r_0 A^{1/3}$ . Thus,  $\bar{l}$  for the sum of the fissioning nuclei will be lowered even more. For fission of lighter nuclei where the transfer reactions do not lead to fission,<sup>6</sup> the value of  $\bar{l}$  for the fissioning nuclei will be approximately that of the compound nuclei that are formed.

These considerations are important in any attempts to analyze fission fragment angular distributions with heavy ions. Because the angular momentum enters into the theoretical interpretation of these distributions as  $\bar{l}^2$ , the uncertainties in the average angular momentum created by the surface reactions affect the conclusions quite strongly. This problem also hinders the treatment

of data from isomer ratios for metastable states formed from heavy-ion systems.

#### ACKNOWLEDGMENTS

The authors are indebted to Albert Ghiorso for his interest and many helpful discussions concerning this work. We are grateful to Homer E. Conzett, Richard M. Diamond, George J. Igo, T. Darrach Thomas, and Bruce D. Wilkins for their assistance in the interpretation of these results. Robert M. Latimer and Walter F. Stockton prepared the excellent silicon detectors, and Charles A. Corum designed the fission chamber. We also thank Roberta B. Garrett and Suzanne M. Hargis for their valuable aid in processing the data. The HILAC crew is acknowledged for excellent beams and other assistance during the experiments.

### Finite Nuclear Size Effects in $\beta$ Decay\*

C. P. BHALLA

*Westinghouse Atomic Power Division, Pittsburgh, Pennsylvania*

AND

M. E. ROSE

*University of Virginia, Charlottesville, Virginia*

(Received May 28, 1962)

The finite nuclear size effects are of significant importance in the study of the second-order corrections to the allowed beta transitions, evaluation of nuclear matrix elements, and in all cases where the  $\xi$  approximation is not valid. Accurate electronic radial functions are computed by considering the finite nuclear size effects and the finite de Broglie wavelength effects. A summary of the computation procedure is given, and a comparison of the calculated beta-decay functions is made with the corresponding Coulomb functions.

#### 1. INTRODUCTION

THE extensive work done in the last three years has led to the general acceptance of the vector and the axial vector interactions for the processes of nuclear beta decay. A considerable interest has developed in the following types of problems: (1) a study of second-order effects, (2) evaluation of nuclear matrix elements, (3) precision measurements of beta polarization, and (4) a detailed analysis of the  $\beta$ - $\gamma$  (circular polarization) correlation experiments. For all these investigations, one needs to know accurate electronic functions, which occur in the theoretical formulas. For example, empirical values of the nuclear matrix elements are obtained by fitting the relevant experiments with the theoretical formulas, and then these can be compared with those computed on the basis of a particular nuclear model.

In the computation of beta decay functions, there are two important effects to be considered: (1) the finite nuclear size effects<sup>1</sup> and (2) the finite de Broglie wavelength effect.<sup>2</sup> The corrections due to the finite nuclear size effects are those arising from a consideration of a charge distribution inside the nucleus. For this purpose, a nucleus is generally considered as a sphere of radius  $1.2A^{1/3}$  F, and of a uniform charge distribution. This is in contrast to a point nucleus, i.e., only Coulomb field potential. As a usual practice, the electronic radial functions are evaluated at the nuclear surface. These electronic radial functions for a finite nucleus can be expressed (outside the nucleus) as a proper combination of the regular and the irregular solutions of the Dirac equation with a Coulomb potential. It turns out that some of the beta decay functions are very sensitive to

\* The contribution of one of us (M.E.R.) was partially supported by the U. S. Atomic Energy Commission.

<sup>1</sup> M. E. Rose and D. K. Holmes, *Phys. Rev.* **83**, 190 (1951). Also see M. E. Rose and D. K. Holmes, Oak Ridge National Laboratory Report ORNL-1022 (unpublished).

<sup>2</sup> M. E. Rose and C. L. Perry, *Phys. Rev.* **90**, 479 (1953).

this admixture of the regular and the irregular Coulomb functions. Such a study for the beta spectrum functions was made by Rose and Holmes.<sup>1</sup> As pointed out by Rose *et al.*,<sup>2</sup> the finite de Broglie wavelength effects can be taken into account if the expansion of the confluent hypergeometric functions, which appear in the Coulomb field solutions, is not terminated by the leading term. The parameter in this series expansion is the product of the beta momentum and the nuclear radius.

In view of the large scale computations required for each isotope, we have prepared tables<sup>3</sup> of the electronic radial functions and the tangents of the phase shifts exclusive of the logarithmic term for the total angular momentum  $j=1/2$  and  $j=3/2$ . The Fermi function is also tabulated. We have neglected the small effects (less than 0.2% for heavy nuclei) due to screening. It is the purpose of this paper to summarize the procedure used in these calculations, and to present a comparison of the "field-sensitive" beta-decay functions with the corresponding Coulomb functions.

## 2. FORMULATION OF THE PROBLEM

Throughout, we use the relativistic rationalized units  $\hbar=m=c=1$ . We express the solution of the Dirac equation,

$$[-\alpha \cdot \mathbf{p} - \beta + V(r)]\psi_\kappa^\mu = W\psi_\kappa^\mu, \quad (1)$$

as

$$\psi_\kappa^\mu = \begin{pmatrix} -i f_\kappa(r) \chi_{\kappa-\mu} \\ g_\kappa(r) \chi_{\kappa\mu} \end{pmatrix}, \quad (2)$$

where a uniform charge distribution inside a nucleus corresponds to a potential  $V(r)$  for an electron:

$$V(r) = -\alpha Z/r \quad \text{for } r > \rho, \\ V(r) = -\frac{\alpha Z}{2\rho} \left( 3 - \frac{r^2}{\rho^2} \right) \quad \text{for } r < \rho. \quad (3)$$

In our units, the nuclear radius  $\rho$  is given as

$$\rho = 0.4285\alpha A^{1/3},$$

where  $\alpha$  is the fine structure constant (1/137.03).  $\chi_{\kappa\mu}$  is the spin-angular function.<sup>4</sup> Also, we have

$$j = |\kappa| - 1/2, \\ l = \kappa \quad \text{for } \kappa > 0, \\ l = -(\kappa + 1) \quad \text{for } \kappa < 0.$$

<sup>3</sup> C. P. Bhalla and M. E. Rose, Oak Ridge National Laboratory Report ORNL-3207, 1962 (unpublished). In these tables  $f_\kappa$ ,  $g_\kappa$ ,  $\tan\Delta_\kappa$  for  $\kappa = \pm 1$  and  $\kappa = \pm 2$  and the Fermi function [Eq. (A8)] are given for 93 values of  $Z$  separately for the electrons and the positrons corresponding to thirty values of beta momentum in steps of 0.2 up to a maximum value of 6.2. Also see C. P. Bhalla and M. E. Rose, Oak Ridge National Laboratory Report ORNL-2954, 1960 (unpublished). In ORNL-2964, the entries under  $\sin\Delta$  should be used with a negative sign for positrons.

<sup>4</sup> M. E. Rose, *Elementary Theory of Angular Momentum* (John Wiley & Sons, Inc., New York 1957).

We take the normalization of  $f_\kappa$  and  $g_\kappa$  to correspond to one particle in a sphere of unit radius. The asymptotic behavior of the electronic radial functions is given by

$$rf_\kappa \rightarrow -\left(\frac{W-1}{W}\right)^{1/2} \sin\left(\frac{\alpha ZW}{p} \ln 2pr + \Delta_\kappa\right), \\ rg_\kappa \rightarrow \left(\frac{W+1}{W}\right)^{1/2} \cos\left(\frac{\alpha ZW}{p} \ln 2pr + \Delta_\kappa\right), \quad (4)$$

where  $W = (p^2 + 1)^{1/2}$ .

For the Coulomb field potential, we represent the solution of the Dirac equation as

$$\psi_\kappa^\mu = \begin{pmatrix} -i(F_\kappa/r)\chi_{\kappa-\mu} \\ (G_\kappa/r)\chi_{\kappa\mu} \end{pmatrix}.$$

The asymptotic behavior of  $F_\kappa(r)$  and  $G_\kappa(r)$  is given by Eq. (4) with  $\Delta_\kappa$  written as  $\delta_\kappa$ , where<sup>5</sup>

$$\delta_\kappa = -\arg\Gamma(\gamma_\kappa + iy) + \eta_\kappa - \frac{1}{2}\pi\gamma_\kappa, \quad (5a)$$

and

$$y = \alpha ZW/p, \quad (5b)$$

$$e^{2i\eta_\kappa} = -\frac{(\kappa - i\alpha Z/p)}{(\gamma_\kappa + iy)}, \quad (5c)$$

$$\gamma_\kappa = [\kappa^2 - (\alpha Z)^2]^{1/2}. \quad (5d)$$

The irregular solutions shall be denoted by  $\bar{F}_\kappa$  and  $\bar{G}_\kappa$ .

We represent by  $F^{(i)}/r$  and  $G^{(i)}/r$  as the regular solution of Dirac equation, Eq. (1), for  $r < \rho$ . We obtain

$$rf_\kappa(r) = AF_\kappa^{(i)}(r), \\ rg_\kappa(r) = AG_\kappa^{(i)}(r), \quad (6)$$

and

$$rf_\kappa(r) = BF_\kappa(r) + C\bar{F}_\kappa(r), \\ rg_\kappa(r) = BG_\kappa(r) + C\bar{G}_\kappa(r). \quad (7)$$

The normalization condition on  $f_\kappa$  and  $g_\kappa$  gives

$$B^2 + C^2 + 2BC \cos(\delta - \bar{\delta}) = 1. \quad (8)$$

The continuity of  $f_\kappa$  and  $g_\kappa$  at  $r = \rho$  gives

$$AF_\kappa^{(i)}(\rho) = BF_\kappa(\rho) + C\bar{F}_\kappa(\rho), \\ AG_\kappa^{(i)}(\rho) = BG_\kappa(\rho) + C\bar{G}_\kappa(\rho). \quad (9)$$

From Eqs. (9), we get

$$A = \left( \frac{F/G - \bar{F}/\bar{G}}{F^{(i)}/G^{(i)} - \bar{F}/\bar{G}} \right) \frac{G_\kappa}{G_\kappa^{(i)}} B \quad (10)$$

and

$$C = \left( \frac{F/G - F^{(i)}/G^{(i)}}{F^{(i)}/G^{(i)} - \bar{F}/\bar{G}} \right) \frac{G_\kappa}{\bar{G}_\kappa} B. \quad (11)$$

In Eqs. (10) and (11), we have put a subscript  $\kappa$  on the

<sup>5</sup> M. E. Rose, Phys. Rev. **51**, 484 (1937).

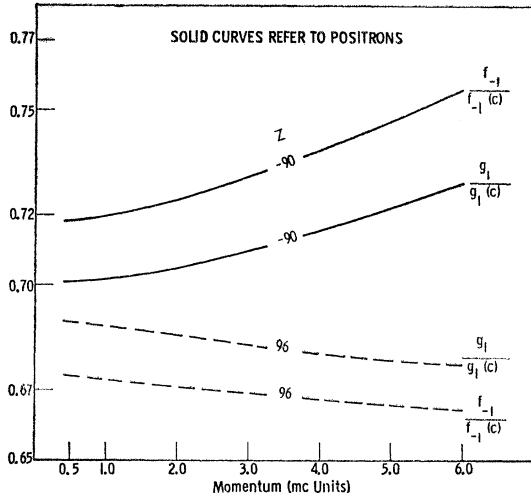


FIG. 1. The ratios of the field sensitive radial functions  $f_{-1}$  and  $g_1$  for  $j=1/2$  to the corresponding Coulomb functions  $f_{-1}(c)$  and  $g_1(c)$  vs beta momentum for electrons ( $Z=96$ ) and positrons ( $Z=90$ ).

parenthesis to imply that all the functions carry a subscript  $\kappa$ . Also, wherever we omit the argument of radial functions, it means that these are evaluated at the nuclear radius  $\rho$ . We define  $H$  by Eq. (11) as

$$C = BH.$$

Eq. (8) gives

$$B = [1 + H^2 + 2H \cos(\delta - \bar{\delta})]^{-1/2}. \quad (12)$$

We obtain from Eqs. (6) and (11)

$$g_{\kappa}(\rho) = B \left( \frac{F/G - \bar{F}/\bar{G}}{F^{(\kappa)}/G^{(\kappa)} - \bar{F}/\bar{G}} \right)_{\kappa} \frac{G_{\kappa}(\rho)}{\rho} \quad (13a)$$

and

$$f_{\kappa}(\rho) = \frac{F_{\kappa}^{(\kappa)}(\rho)}{G_{\kappa}^{(\kappa)}(\rho)} g_{\kappa}(\rho). \quad (13b)$$

In our calculations, we compute  $f_{\kappa}(\rho)$  and  $g_{\kappa}(\rho)$  from Eqs. (13). The formula for the tangent of the asymptotic phase, exclusive of the logarithmic term, is given by Eq. (A1) of Appendix A.

### 3. NUMERICAL RESULTS

In Fig. 1, we give the ratios of  $f_{-1}$  and  $g_1$  to the corresponding Coulomb functions  $f_{-1}(c)$  and  $g_1(c)$  as a function of beta momentum. The dashed and the solid curves refer to electrons for  $Z=96$  and positrons for  $Z=90$ , respectively. Similar plots are shown for  $j=3/2$  (i.e.,  $\kappa = \pm 2$ ) in Fig. 2. The finite nuclear size corrections reduce the electronic radial functions for  $j=1/2$  by approximately 30% for heavy nuclei. This is in contrast to a reduction of  $f_{-2}$  and  $g_2$  (for  $j=3/2$ ) by approximately 10%. As is to be expected, the finite nuclear size corrections to the electronic radial functions decrease with higher angular momentum and with lower

values of  $Z$ . Explicit calculations show that these corrections<sup>6</sup> are negligible for  $f_1$ ,  $f_2$ ,  $g_{-1}$ , and  $g_{-2}$ .

For purposes of illustration, we consider only those beta-decay functions which contain one or more of the following:  $f_{-1}$ ,  $g_1$ ,  $f_{-2}$ , and  $g_2$ . In beta polarization,<sup>7</sup> the following combinations occur:

$$B_0 = (\rho^2 F_0 \rho^2)^{-1} f_{-1} g_1 \sin(\Delta_1 - \Delta_{-1}), \quad (14a)$$

$$D_0 = (\rho^2 F_0 \rho)^{-1} (f_1 f_{-1} - g_1 g_{-1}) \sin(\Delta_1 - \Delta_{-1}). \quad (14b)$$

In  $\beta$ - $\gamma$  (circular polarization) correlation formulas, we have<sup>8</sup>

$$N_{12} = (2\rho^2 F_0 \rho)^{-1} [f_{-1} f_2 \cos(\delta_{-1} - \delta_2) + g_1 g_{-2} \cos(\delta_1 - \delta_{-2})]. \quad (14c)$$

In Eqs. (14),  $F_0$  is the Fermi function. We define  $\Delta B_0$  by Eq. (15).

$$\Delta B_0 = [B_0 - B_0(c)] / B_0(c). \quad (15)$$

In Eq. (15),  $B_0(c)$  is computed for a Coulomb field potential. Similarly, we define  $\Delta D_0$  and  $\Delta N_{12}$ .

In Fig. 3,  $\Delta B_0$  and  $\Delta D_0$  are plotted as a function of beta momentum for electrons and positrons.  $\Delta N_{12}$  is given as a function of beta momentum in Fig. 4. The dashed and the solid curves refer to electrons and positrons, respectively. For electrons we take  $Z=50$ , 84, and 96, whereas for positrons we have taken  $Z=39$ , 57, and 90. Similar curves for beta spectrum functions are given by Rose and Holmes<sup>1</sup>.

### 4. DISCUSSION AND CONCLUSIONS

To understand these numerical results, we examine the indicial behavior of the radial functions for a central

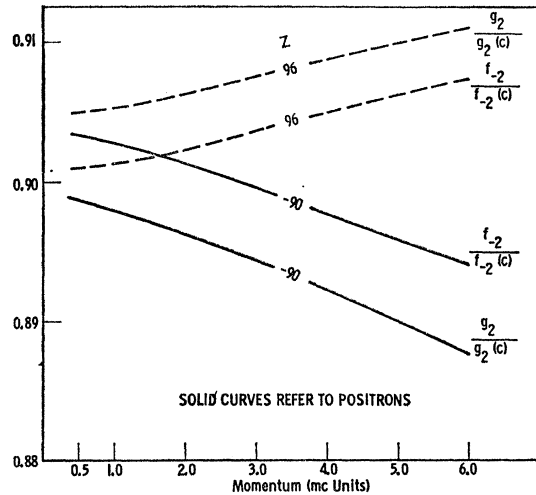


FIG. 2. The ratios of the radial functions  $f_{-2}$  and  $g_2$  for  $j=3/2$  to the corresponding Coulomb functions  $f_{-2}(c)$  and  $g_2(c)$  vs beta momentum for electrons ( $Z=96$ ) and positrons ( $Z=90$ ).

<sup>6</sup> For heavy nuclei the  $\beta^-$  radial functions  $f_1$  and  $g_{-1}$  are reduced at the most by 6% in contrast to a reduction of  $f_2$  and  $g_{-2}$  by one percent.

<sup>7</sup> C. P. Bhalla and M. E. Rose, Phys. Rev. 120, 1415 (1960).

<sup>8</sup> M. Morita and R. S. Morita, Phys. Rev. 109, 2048 (1958).

field potential, as given by Rose.<sup>9</sup> For convenience, we use the same notation:

$$k = |\kappa|, \quad X = r/\rho, \quad \text{and} \quad W(X) = (2j+2)X^{2j+1},$$

$$g_k \sim C_1(2j+2)^{-1}\rho^{j+3/2} \int_0^1 V(X)W(X)dX,$$

$$\text{and} \quad f_k \sim C_1\rho^{j+1/2} \quad \text{for} \quad \kappa > 0, \quad (16a)$$

$$g_{-k} \sim C_2\rho^{j+1/2},$$

$$f_{-k} \sim C_2(2j+2)^{-1}\rho^{j+3/2} \int_0^1 V(X)W(X)dX \quad \text{for} \quad \kappa < 0. \quad (16b)$$

In Eqs. (16),  $C_1$  and  $C_2$  are constants. It is clear that  $g_k$  and  $f_{-k}$  are the "field-sensitive" functions, because they contain an average of the field potential with  $W$  as a weighting factor. On the other hand, the indicial behavior of  $g_{-k}$  and  $f_k$  is essentially governed by the angular momentum considerations. However, since the integrals in Eqs. (16) approach delta functions for large values of angular momentum, the finite nuclear size effects are negligible in such a case. These observations are confirmed by the numerical work.

At this point, some remarks about the choice of a phase convention used in the computations of radial functions are pertinent. In the evaluation of  $G_\kappa$  from Eq. (A7), there is an ambiguity in the choice of quadrant for  $\eta_\kappa$  because only  $\exp(2i\eta_\kappa)$  is given by Eq. (5c). No such difficulty arises in the computations of the ratios of the radial functions which appear in Eqs. (13). However, all combinations of the radial functions and sines or cosines of the difference in phase shifts, which occur

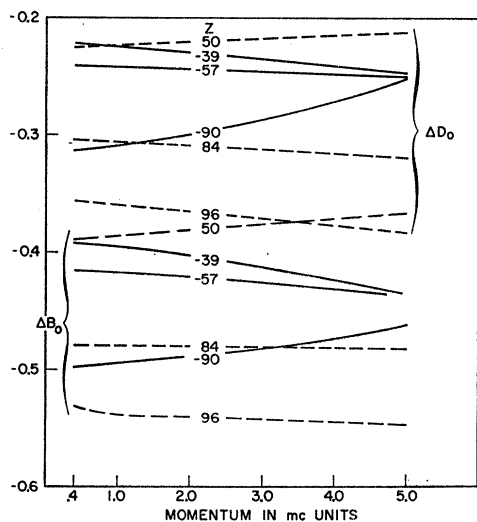


FIG. 3. Correction factors for beta polarization functions  $B_0$  and  $D_0$  vs beta momentum for electrons (dashed curves) and for positrons (solid curves). The numbers attached to the curves refer to the values of  $Z$  used in Eq. (3) of the text.

<sup>9</sup> M. E. Rose, Phys. Rev. **82**, 389 (1951).

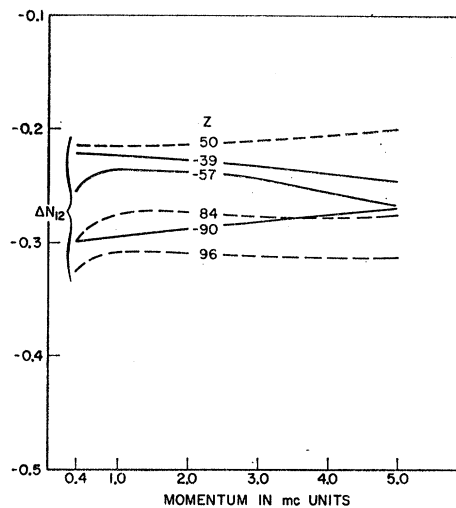


FIG. 4. Correction factor for  $N_{12}$  vs beta momentum for electrons (dashed curves) and for positrons (solid curves). The numbers attached to the curves refer to the values of  $Z$  used in Eq. (3) of the text.

in the theoretical formulas, are independent of any choice of this phase convention.

The numerical results presented in this paper show that the beta decay functions, which are multiplied by the appropriate nuclear matrix elements in the theoretical formulas, are affected depending upon whether or not these functions contain the field sensitive radial functions. The nuclear matrix elements are considered as parameters in the standard treatment, and these are determined by a comparison of the experimental data with the relevant theoretical formulas. Therefore, the finite nuclear size effects should be taken into account in this empirical evaluation of the nuclear matrix elements. Generally, one can compare these empirical values with those obtained from a nuclear model.<sup>10</sup>

In the study of second-order effects in the allowed beta transitions, accurate functions must be used because otherwise these very small effects would be obliterated. Similarly, whenever there is a cancellation of the leading terms in the theoretical formulas, approximate beta decay functions are not adequate.

In conclusion, since the tables of accurately calculated electronic functions are available,<sup>3</sup> these could be used profitably and conveniently in the analysis of beta decay experiments.

#### ACKNOWLEDGMENTS

One of us (C. P. B.) wishes to express his appreciation to the National Bureau of Standards for part financial support, and to the administration of the Oak Ridge National Laboratory for their hospitality and the Computer facilities.

<sup>10</sup> M. E. Rose and R. K. Osborn, Phys. Rev. **93**, 1326 (1954). Also see T. Ahrens and E. Feenberg, Phys. Rev. **86**, 64 (1952) and D. L. Pursey, Phil. Mag. **42**, 1193 (1951).

APPENDIX A

The tangent of the asymptotic phase, exclusive of the logarithmic term, is given by the following:

$$\tan\Delta_\kappa = \frac{-a_0 + a_1 \tan\eta_\kappa + H_\kappa(\cos\bar{\eta}/\cos\eta)_\kappa(a_2 + a_3 \tan\bar{\eta}_\kappa)}{a_1 + a_0 \tan\eta_\kappa + H_\kappa(\cos\bar{\eta}/\cos\eta)_\kappa(a_3 - a_2 \tan\bar{\eta}_\kappa)}, \tag{A1}$$

where

$$\begin{aligned} a_0 &= a_4 \sin(\pi\gamma_\kappa/2) + a_5 \cos(\pi\gamma_\kappa/2), \\ a_1 &= a_4 \cos(\pi\gamma_\kappa/2) - a_5 \sin(\pi\gamma_\kappa/2), \\ a_2 &= a_6 \sin(\pi\gamma_\kappa/2) - a_7 \cos(\pi\gamma_\kappa/2), \\ a_3 &= a_6 \cos(\pi\gamma_\kappa/2) + a_7 \sin(\pi\gamma_\kappa/2), \\ a_4 &= \operatorname{Re} \frac{\Gamma(\gamma_\kappa + iy)}{|\Gamma(\gamma_\kappa + iy)|}, & a_5 &= \operatorname{Im} \frac{\Gamma(\gamma_\kappa + iy)}{|\Gamma(\gamma_\kappa + iy)|}, \\ a_6 &= \operatorname{Re} \frac{\Gamma(-\gamma_\kappa + iy)}{|\Gamma(-\gamma_\kappa + iy)|}, & a_7 &= \operatorname{Im} \frac{\Gamma(-\gamma_\kappa + iy)}{|\Gamma(-\gamma_\kappa + iy)|}. \end{aligned}$$

The ratios of the radial functions were computed from the following set of equations. In the following, we omit the subscript  $\kappa$  on  $\gamma_\kappa$ .

$$(F/G)_\kappa = (\gamma + \kappa/\alpha z) (\sum_n S_n / \sum_n T_n)_\kappa, \tag{A2}$$

where

$$S_0 = T_0 = 1$$

and

$$S_n = -\frac{\alpha Z \rho}{n(n+2\gamma)} \left[ \frac{(W-1)(\gamma+n+\kappa)}{\kappa+\gamma} T_{n-1} + (W+1)S_n \right], \tag{A3}$$

$$T_n = \frac{\alpha Z \rho}{n(n+2\gamma)} \left[ \frac{(W+1)(\gamma+n-\kappa)}{\kappa-\gamma} S_{n-1} - (W-1)T_{n-1} \right]. \tag{A4}$$

$(\bar{F}/\bar{G})_\kappa$  is obtained by changing  $\gamma$  to  $-\gamma$  in Eqs. (A2), (A3), and (A4).

$$\left( \frac{G}{\bar{G}} \right)_\kappa = \sigma \frac{\sum_n T_n}{\sum_n \bar{T}_n}, \tag{A5}$$

where  $\bar{T}_n$  is computed from (A4) by replacing  $\gamma$  by

$-\gamma$  and

$$\sigma \equiv (2\phi\rho)^{2\gamma} \frac{|\Gamma(\gamma+iy)|}{|\Gamma(-\gamma+iy)|} \frac{\Gamma(1-2\gamma)}{\Gamma(1+2\gamma)} \left[ \frac{\Gamma(W\gamma-\kappa)(\kappa-\gamma)}{(W\kappa+\gamma)(\kappa+\gamma)} \right]^{1/2}.$$

$F^{(i)}/G^{(i)}$  was computed from the following equation for  $\kappa < 0$ :

$$(F^{(i)}/G^{(i)})_\kappa = \rho (\sum_n b_n / \sum_n b'_n), \tag{A6}$$

where

$$\begin{aligned} b'_0 &= 1, & b_0 &= -(2|\kappa|+1)^{-1}(W-1+3\alpha Z/2\rho), \\ b_n &= \left[ -\left( W-1 + \frac{3\alpha Z}{2\rho} \right) b'_n + \frac{\alpha Z}{2\rho} b'_{n-1} \right] (2n+2|\kappa|+1)^{-1}, \\ b'_n &= \frac{\rho^2}{2n} \left[ \left( W+1 + \frac{3\alpha Z}{2\rho} \right) b_{n-1} - \frac{\alpha Z}{2\rho} b_{n-2} \right]. \end{aligned}$$

For  $\kappa > 0$ ,  $F_\kappa^{(i)}/G_\kappa^{(i)}$  was obtained from Eq. (A6) by interchanging  $F^{(i)}$  and  $G^{(i)}$  and changing the signs of  $W$  and  $Z$ .

In the computations of  $\sum_n S_n / \sum_n T_n$ ,  $\sum_n T_n / \sum_n \bar{T}_n$ ,  $\sum_n \bar{S}_n / \sum_n \bar{T}_n$ , and  $\sum_n b_n / \sum_n b'_n$ , the series was terminated when the contribution of the terms was less than  $10^{-6}$ . The complex gamma function and the real gamma function were also computed to this accuracy.

$G_\kappa$  was computed from the following equation:

$$\begin{aligned} G_\kappa &= \frac{(1+W)^{1/2}}{W^{1/2}} (2\phi\rho)^\gamma e^{\pi y/2} \frac{|\Gamma(\gamma+iy)|}{\Gamma(1+2\gamma)} \\ &\times \frac{1}{2} [e^{-i\nu\rho+iy} {}_1F_1(\gamma+1+iy, 2\gamma+1, 2i\phi\rho) + \text{c.c.}], \end{aligned} \tag{A7}$$

where the confluent hypergeometric function can be represented by the series

$${}_1F_1(a, b, Z) = \frac{\Gamma(b)}{\Gamma(a)} \sum_{m=0}^{\infty} \frac{\Gamma(a+m)}{\Gamma(b+m)} \frac{Z^m}{m!},$$

over the entire complex plane  $|Z| < \infty$ . In the evaluation  $G_\kappa$ , the terms in the series were terminated, when two consecutive terms were less than  $10^{-6}$ .

The Fermi function,  $F_0$ , was calculated from

$$F_0(W, z) = 4(2\phi\rho)^{2(\gamma_1-1)} e^{\pi v} \left( \frac{|\Gamma(\gamma_1+iy)|}{\Gamma(2\gamma_1+1)} \right)^2. \tag{A8}$$